# Proposal of a Fermi–Dirac-Derived Reactivity Descriptor: Beyond the Frontier MO Model

R. Moulandou-Koumba, M. Doggui, S. N'sikabaka, J.-M. Ouamba, Y. Arfaoui, G. Frapper, Frédéric Guégan

# Proposal of a Fermi-Dirac Derived Reactivity Descriptor: Beyond the Frontier MO Model

R. D. Moulandou-Koumba,[†,‡] M. Y. Doggui,[†,¶] S. N'Sikabaka,[‡] J.-M. Ouamba,[‡] Y. Arfaoui,[¶] G. Frapper,[†] and F. Guégan[*,†]

†*IC2MP UMR 7285, Université de Poitiers – CNRS, 4, rue Michel Brunet TSA 51106–86073 Cedex 9 Poitiers, France.*

‡*Université Marien NGOUABI, Faculté des Sciences et Techniques, Unité de Chimie du Végétal et de la Vie, BP 69 Brazzaville, Congo*

¶*Laboratory of Characterizations, Applications & Modeling of Materials (LR18ES08), Department of Chemistry, Faculty of Sciences, University of Tunis El Manar, 2092 Tunis – Tunisia*

E-mail: frederic.guegan@univ-poitiers.fr

## Abstract

In this paper, we derive a reactivity descriptor stemming from the Fermi-Dirac population scheme, applied to density functional calculations on molecular systems. Assuming molecular orbitals only marginally change when temperature is slightly increased from 0 K, we study the response of electron density to a change in temperature. Connection with usual conceptual DFT descriptors is made, and the T-variation of electron density for some representative examples is given and discussed.

# Introduction

Predicting and rationalising chemical reactivity is one of the central concerns in theoretical chemistry. To address it, various frameworks were proposed over time. These frameworks often rely on a so-called "perturbation perspective":[1] the approach of a reagent towards another can be seen as a perturbation of the latter in its resting state. This holds for the early stages of reaction (weak interaction), and may be extended further provided that the Hammond's postulate holds.[2]

Hence one may try to extract meaningful chemical information from a given system by probing its response to external perturbations. In C-DFT, this is usually achieved by analysing electron density and energy variations against two central variables: the external potential, $v(\mathbf{r})$, and either the total number of electrons N (in the so-called canonical development) or the chemical potential $\mu$ (grand-canonical approach).[3,4]

Nevertheless, responses to other types of perturbations can be conceived.[5] For instance, recently the group of F. de Proft studied the responses of various systems to electric fields[6] and external mechanical force.[7] New descriptors may thus be constructed, and they are expected to afford deeper and finer insight on chemical properties. Sometimes, as we will show in the following paragraphs, the mathematical development of these descriptors furthermore shows strong connection between these original quantities and previously proposed ones. Hence the derivation of new descriptors is also of interest to develop and strengthen our understanding of well-established theories and models.

Inclusion of temperature in C-DFT is of course of particular interest. Several proposals were made in the past years, either relying on the definition of DFT-derived temperature[8–11] or on the use of temperature as an additional external variable in DFT, using ensemble approaches.[12–21] Original descriptors and quantities were derived in these conditions, and satisfactorily afford to retrieve long-known quantities in the zero-K limit. However, some descriptors are ill-behaved in this 0 K limit (Dirac delta distribution behaviour). Additionally, the use of ensemble state calculations is slightly cumbersome, and one may wonder whether

a more approximate though simpler model could not be devised.

Here, we propose a simple approach to incorporate temperature dependence in a C-DFT like approach. Our proposition relies on the following hypothesis: provided that temperature is low, the Kohn Sham orbitals obtained from "standard" 0 K calculation are a good approximation of the T-dependent ones, and the effect of temperature is principally to alter their population (Fermi-Dirac population scheme).[22] Under these conditions, we develop the first order response of electron density to a change in temperature, details of the development being given in section 2, special attention being given to the derivation of a normalised response. Such a quantity is expected to provide valuable information on reactivity. Indeed, in a recent publication it was proposed that intermolecular interaction can be divided into "heat" and "work" exchange between reagents.[23] Probing how an electron density can vary according to a change in temperature, that is under a heat exchange with an external partner or reservoir, is thus of interest. In section 3, computational details are provided (note the code is given in SI). In the fourth section, we illustrate the potential of the proposed descriptors on prototypical systems, some of them being hard to study through standard approximations, as a consequence of frontier MO degeneracy. The paper ends on concluding remarks.

# Theory

## Initial development

The central idea of the development is to use a Fermi-Dirac population scheme on molecular orbitals from SCF calculations: instead of integer (2 or 0) occupations, let us write that the molecular orbital i bears $n_i$ electrons according to:

$$n_i(T) = \frac{2}{1 + \exp\left(\frac{\varepsilon_i - \mu}{k_B T}\right)} \tag{1}$$

where $k_B$ is the Boltzmann constant, T the temperature, $\varepsilon_i$ the MO energy, and $\mu$ the chemical potential. As noted by Parr and Yang, this is actually exact for a system of non-interacting electrons (Kohn-Sham like construction).[24]

If the system under study is a pure, macroscopic sample of a given compound, then we may expect that the chemical potential $\mu$ is the average chemical potential of an individual molecule,

$$\mu = \left(\frac{\partial E}{\partial N}\right)_{v(\mathbf{r})} \tag{2}$$

which can also be seen as the average of the frontier levels energies.[25]

One may already note that under such conditions the total number of electrons $\langle N \rangle$ (sum of $n_i$) will differ from the expected value N, unless the MO distribution is symmetrical around $\mu$. Deviations may nonetheless be rather small at low T, and if T tends to zero $\langle N \rangle$ tends to N, since the Fermi-Dirac distribution tends towards a Heaviside distribution.[a]

The average electron density should then be:

$$\tilde{\rho}(\mathbf{r}, T) = \sum_{i=1}^{N'} n_i(T) |\varphi_i(\mathbf{r})|^2 \tag{3}$$

with $\varphi_i$ the MO associated to $\varepsilon_i$. It must already be noted that this is an approximation of the correct temperature-dependent electron density, since here we use the T=0 K molecular orbitals (and not MOs from a T-dependent SCF calculations)[24], and no entropy contribution is considered.[26] Nevertheless, if temperature remains small, this approximation should remain correct, and in the same line of arguments as before, $\tilde{\rho}$, the 0 K SCF electron density and the genuine T-dependent electron density should be nearly equal.

Thus one may expect to extract some temperature-dependence effects from equation 3, which can be rather straightforwardly evaluated from any SCF calculation output. Indeed,

[a] In fact, a numerical experiment on a benzene molecule at T = 2500 K reveals that $\langle N \rangle$ and N differ by about $1.10^{-9}$, suggesting that 2500 K is a "low" temperature here.

from Equations 1 and 3, one may then compute the response of electron density to a change in temperature:

$$f_T(\mathbf{r}) = \left(\frac{\partial \tilde{\rho}_N(\mathbf{r},T)}{\partial T}\right)_{v(\mathbf{r}),\mu} = \sum_{i=1}^{N'} \left(\frac{\partial n_i(T)}{\partial T}\right)_{v(\mathbf{r}),\mu} |\varphi_i(\mathbf{r})|^2 \tag{4}$$

assuming the orbital temperature-dependent relaxation remains small enough to be neglected. From the previous equations one directly obtains that

$$f_T(\mathbf{r}) = 2\sum_{i=1}^{N'} \left(\frac{\varepsilon_i - \mu}{k_B T^2}\right) \exp\left(\frac{\varepsilon_i - \mu}{k_B T}\right) \left[1 + \exp\left(\frac{\varepsilon_i - \mu}{k_B T}\right)\right]^{-2} |\varphi_i(\mathbf{r})|^2 \tag{5}$$

$$= \sum_{i=1}^{N'} n_i'(T) |\varphi_i(\mathbf{r})|^2 \tag{6}$$

The $n_i'(T)$ coefficients present several noticeable features.

First, from equation 5 it may be noted that degenerate MOs will be associated to the same value of $n_i'$ (only depending on energies), so the proposed descriptor naturally incorporates some degeneracy effects.[b] Second, it may be noted that $n_i'$ is an odd function of $\varepsilon_i - \mu$ (saying otherwise, $n_i'$ is antisymmetric around $\mu$), adopting negative values for occupied MOs ($\varepsilon_i < \mu$) and positive values otherwise. Third, the further away from the Fermi level, the smaller the absolute value of $n_i'$, which quickly converges to zero far from $\mu$. As a consequence, maximal contributions are expected for MOs around the Fermi level, in correspondence with the frontier MO model:[28] the principal response of the electron density to a change in temperature, that is, to an energy transfer, stems from the frontier and near frontier MOs.

Actually, let us assume the system under study is such that the frontier MOs (HOMO and LUMO) are well-separated from all other MOs. In such a case, the two principal contributions to the electron density variation with temperature will stem from these two MOs. Using usual C-DFT notations and approximations,[29,30] we have $\varepsilon_{HO} = \mu - \eta/2$ and

[b] Although it must be reminded that, owing to our premises, static correlation is missing in our development. As pointed out by a referee, a more complete treatment of degeneracy requires much more complete and complex developments.[13,27]

$\varepsilon_{LU} = \mu + \eta/2$, and thus one has:[c]

$$f_T(\mathbf{r}) \approx -\frac{\eta \exp\left(-\frac{\eta}{2k_BT}\right)}{k_BT^2\left(1+\exp\left(-\frac{\eta}{2k_BT}\right)\right)^2}|\varphi_{HO}(\mathbf{r})|^2 + \frac{\eta \exp\left(\frac{\eta}{2k_BT}\right)}{k_BT^2\left(1+\exp\left(\frac{\eta}{2k_BT}\right)\right)^2}|\varphi_{LU}(\mathbf{r})|^2 \quad (7)$$

$$\approx \frac{\eta}{k_BT^2}\exp\left(-\frac{\eta}{2k_BT}\right)\left(|\varphi_{LU}(\mathbf{r})|^2 - |\varphi_{HO}(\mathbf{r})|^2\right) \quad (8)$$

$$= \frac{\eta}{k_BT^2}\exp\left(-\frac{\eta}{2k_BT}\right)\Delta f(\mathbf{r}). \quad (9)$$

In the previous equation, $\Delta f(\mathbf{r})$ is the so-called Dual Descriptor[31,32], here evaluated under the Frontier MO (FMO) approximation. A comparable formula was actually obtained by Franco-Perez and co-workers,[18,33] using a three-states ensemble model to describe the temperature response of electron density. The apparition of the dual descriptor is thus not a complete surprise, but it is nonetheless interesting to observe that this "second-order" electron density response (with respect to the number of electrons or chemical potential, in 0 K developments)[3] is an avatar of a first order response at finite temperature. The first-order response of electron density to a change in temperature will thus bear close resemblance to the dual descriptor, and may actually be seen as a generalisation of the latter.[d] Satisfactorily, one may note the explicit dependence on hardness in the electron density response: at a given temperature, the higher $\eta$, the smaller the prefactor, and thus the lower the electron density variation. This is in perfect line with expectations from Pearson's HSAB theory[34] and the principle of maximum hardness.[35] Now it must be noted that though the right hand side of Equation 9 integrates to zero, the same is not true in general for the electron density response to temperature - in fact, this condition will be true only if the distribution of MO energies around the Fermi level is symmetric.

It is also noteworthy that beyond the FMO approximation, equation 6 indicates that other than frontier MOs may contribute, especially when temperature increases (larger width of the

[c] Assuming temperature is low ($\eta/k_BT >> 1$), which allows to approximate both denominators in Equation (7).

[d] It may additionnally be added that, as electron density is itself a first order response of electron density, all descriptors in the previous statement are "one order higher" with respect to energy.

$n_i'$ function). In line with a previous statement, we can thus see the first-order response of $\rho$ to a change in temperature as a generalisation of the dual descriptor beyond the classical FMO approximation, in the spirit of the recent proposition of B. Pino-Rios.[36] In this study, the authors proposed to generalise the FMO dual descriptor through an expansion over all MOs, weighting each MO contribution using a Gaussian scheme based on the energy difference with respect to the frontier levels. Here, the weighting is not Gaussian, but similarly it decays quickly as MOs are further away from the chemical potential, and thus from the frontier level – also in line with a previous proposition by C. Cardenas and co-workers.[37] Temperature in our proposition plays a comparable role with the Gaussian distribution width $\Delta$ in B. Pino-Rios proposition: by playing on this value, contributions from deeper MOs can be incorporated or reduced to zero.[e] Note the same

In fact, if temperature is high enough, the maximal contributions in Equation 5 may even stem from non-frontier MOs. Using the explicit dependence over $\varepsilon_i$ in the previous equation, we can find the extrema of $n_i'$ at a given temperature. Indeed, from

$$\frac{\partial n_i'(T)}{\partial \varepsilon_i} = \frac{\left((\varepsilon_i - \mu)\tanh\left(-\frac{\varepsilon_i-\mu}{2k_BT}\right) + k_BT\right)\operatorname{sech}^2\left(-\frac{\varepsilon_i-\mu}{2k_BT}\right)}{2k_B^2T^3} \tag{10}$$

the following condition is expected to hold for extrema

$$\tanh\left(\frac{\varepsilon_i - \mu}{2k_BT}\right) = \frac{k_BT}{\varepsilon_i - \mu} \tag{11}$$

or $\tanh(x/2) = 1/x$ with $x = (\varepsilon_i - \mu)/k_BT$. Though the exact solution of the previous equation is not trivial, numerically one eventually obtains that $x \approx \pm 1.5434$. Here it seems more

[e] In fact, temperature also modulates the magnitude of the electron density reshuffling, as is obvious by Equation 9. Numerical experiments reveal (as shown hereafter) that a temperature nearing 0.1 $\eta$ is required to obtain significant isosurfaces at 0.01 a.u.

natural to consider positive temperatures[f], and thus the contribution of MO i is extremal if

$$\varepsilon_i - \mu \approx 1.5434 k_B T. \tag{12}$$

Temperature may then be chosen so that a given MO i will present the largest contribution to the electron density response. In fact, we can define a particular temperature $T_p$ such that the extrema match the frontier levels:

$$T_p = \frac{\eta}{3.0868 k_B}. \tag{13}$$

Above this temperature, maximal contributions are not necessarily associated to frontier MOs, but may stem from deeper/higher MOs. On the contrary, below this temperature frontier MOs are the principal contributors to the electron density response. It must be noted that $T_p$ is actually already a rather high temperature; for instance in the case of benzene (see below for the calculation details), the calculated hardness is 0.246 a.u., and thus the corresponding $T_p$ is approximately 25 000 K. This temperature is already too high for our approximations to remain valid,[g] so in the following we will restrict our discussion only to $T < T_p$.

## Normalisation

As stated above, in the Fermi-Dirac population scheme no restriction is applied to the total number of electrons $\langle N \rangle$. As a consequence, the electron density is not exactly equal to the 0 K Kohn-Sham density, and its T-derivative is not integrating to zero over all space - meaning the system may acquire or lose electrons under a change in temperature.

Thus formally speaking the quantity derived in equation 6 is a grand-canonical quantity. Usually in C-DFT the grand-canonical descriptors are closely associated to canonical

[f]Though negative temperatures can be conceived for non-equilibrated sub-parts of a given system.

[g]Occupation of the LUMO according to the Fermi-Dirac distribution is indeed equal to 0.35 at this temperature, thus significantly departing from 0.

counterparts, and one may wonder how a canonical (thus with constant total population) equivalent could be derived.

This can be achieved through a slight modification of the Fermi-Dirac population scheme. Let us define a modified coefficient $d_i$ for the MO i, such that overall the total electron count amounts to N:

$$d_i(T) = \frac{N}{\sum_j n_j(T)} n_i(T). \tag{14}$$

From this point, a normalised electron density is straightforwardly derived as

$$\tilde{\rho}_N(\mathbf{r}, T) = \sum_{i=1}^{N'} d_i(T) |\varphi_i(\mathbf{r})|^2. \tag{15}$$

Then the first order T-derivative directly reads

$$f_T(\mathbf{r}) = \left( \frac{\partial \tilde{\rho}_N(\mathbf{r}, T)}{\partial T} \right)_{v(\mathbf{r}),\mu} = \sum_{i=1}^{N'} \left( \frac{\partial d_i(T)}{\partial T} \right)_{v(\mathbf{r}),\mu} |\varphi_i(\mathbf{r})|^2 \tag{16}$$

once again assuming the orbital relaxation remains negligible. Expanding the derivative results in

$$f_T(\mathbf{r}) = = \frac{N}{\left[ \sum_{j=1}^{N'} n_j(T) \right]^2} \left[ \sum_{i=1}^{N'} \left( n_i'(T) \sum_{j=1}^{N'} n_j(T) - n_i(T) \sum_{j=1}^{N'} n_j'(T) \right) |\varphi_i(\mathbf{r})|^2 \right] \tag{17}$$

$$= \sum_{i=1}^{N'} \gamma_i(T) |\varphi_i(\mathbf{r})|^2. \tag{18}$$

As one can note, this quantity indeed integrates to 0 over all space, as expected. Also, one may note the cross product of the Fermi-Dirac coefficients and their first-order T-derivative. Because of this, it is more complicated to delineate mathematical properties for $\gamma$. Nevertheless, we may observe that for deep occupied MOs (far away from the Fermi level) and at

low temperature, the first term is expected to tend to 0 as $n_i'$ does, and thus the second term only should remain. This latter term is expected to be the same for all low-lying MOs, $n_i$ tending to its limit value (2.0) and the sum being a constant. Thus all low-lying MOs will present a comparable contribution to the overall response, which should be small at low T (because the sum of the first order coefficients will be).

On the contrary, for high-lying MOs the second term in equation 17 should vanish ($n_i \to 0$), and so should the first one ($n_i' \to 0$). Thus all high-lying MOs will not contribute to the overall electron density response.

The picture is less clear for near frontier levels. However we may assume that the sum of the first order derivatives $n_i'$ will be small (tending to zero), while the individual contributions themselves could be arbitrarily large near the Fermi level. Thus it may be surmised that the second term in equation 6 will likely be negligible compared to the first one, and only act as a small correction of the latter. Hence around the Fermi level the $\gamma_i$ function should bear close resemblance to $c_i'$, and the conclusions from previous section should remain qualitatively valid.

# Computational details

The electronic structure calculations for all presented examples below were performed using Gaussian 16 rev B.01.[38] In all cases, full geometry optimisations without symmetry constraint were performed in gas phase, and vibrational frequencies calculated to ensure the geometries were actual minima on the potential energy surface. Additional keywords were used to print basis set and MO details in output files[h]. All calculations were performed at the hybrid B3LYP/cc-pvtz level of theory.[39,40]

Descriptors in equations 6 and 17 were then computed using a Python 3/Orbkit[41] script (available in SI) and exported in cube format. Cube dimensions were adapted to each molecule (7.5 bohr extension), and a grid spacing of 0.15 bohr was used in all cases but $C_{60}$,

[h] `iop(6/7=3) gfinput`

for which a larger spacing was used (0.20 bohr) to alleviate the computational effort. In order to limit computational time (and memory requirements), a cut-off was also set up on the values of $n'_i$: all MOs leading to $|n'_i| < 10^{-10}$ were rejected. This allows for a fast computation of the descriptors, even in the case of $C_{60}$ (20 over 1800 MOs used in computation, 3 minutes 30 seconds on 24 cpu).

# Illustration on representative examples

## The cases of benzene and HCN: detailed discussion

Let us first consider the example of the benzene molecule. We give in Table 1 the values for the normalised and non-normalised responses for this molecule at 0.1 Tp (2520 K), for the near-frontier (from HO-3 to LU+3) and extreme MOs. The values of the Fermi-Dirac populations for the same MOs at the same temperature are also given for the sake of comparison.

As said before, though seemingly high, the temperature can be considered "low" in the sense that the Fermi-Dirac population scheme sticks very closely to the expected finite occupations. The strongest deviation, observed for the frontier MOs, amounts to roughly $\pm 4.10^{-7}$ electron. Hence the impact of T at 0th order is extremely weak, if not negligible. This remains true when summing over all 264 MOs: the difference between N and $\langle N \rangle$ is $1.10^{-9}$ electron only.

If we now turn to the non-normalised response, the picture is quite different. As one may judge from the values in Table 1, $n_i$ values are 3 orders of magnitude higher than $\Delta_{int}$ (difference between the occupations in the Fermi-Dirac scheme and expected integer values). Hence, the effect of temperature is more pronounced on the first order derivative. It may further be noticed that the largest contributions, as expected, arise from the frontier MOs (3-4 orders or magnitude difference between HO and HO-3/LU and LU+3 for instance). Satisfactorily, symmetrical values for the degenerate MOs of benzene (HO and HO-1, LU and LU+1) are further retrieved. Ultimately, the non-normalised response principally stems

Table 1: Results of the temperature-dependent calculation for the benzene molecule à 0.1 $T_p$. FD is the Fermi-Dirac coefficient, $\Delta_{int}$ the difference between the Fermi-Dirac and expected integer MO population, $n_i$ the non-normalised first-order T-derivative of the Fermi-Dirac coefficients, and $\gamma_i$ the normalised response. Asterisks indicate that the value was too small to be computed (below cut-off).

| MO | FD | $\Delta_{int}$ | $n_i$ | $\gamma_i$ |
|---|---|---|---|---|
| 1 | 2.00 | 0* | 0* | -3.27 $10^{-6}$ |
| HO-3 | 2.00 | 5.33 $10^{-12}$ | -1.78 $10^{-08}$ | -4.02 $10^{-06}$ |
| HO-2 | 2.00 | 5.34 $10^{-12}$ | -1.78 $10^{-08}$ | -4.02 $10^{-06}$ |
| HO-1 | 2.00 | 3.96 $10^{-07}$ | -7.67 $10^{-04}$ | -3.22 $10^{-02}$ |
| HO | 2.00 | 3.96 $10^{-07}$ | -7.67 $10^{-04}$ | -3.22 $10^{-02}$ |
| LU | 3.96 $10^{-07}$ | -3.96 $10^{-07}$ | 7.67 $10^{-04}$ | 3.22 $10^{-02}$ |
| LU+1 | 3.96 $10^{-07}$ | -3.96 $10^{-07}$ | 7.67 $10^{-04}$ | 3.22 $10^{-02}$ |
| LU+2 | 6.09 $10^{-10}$ | -6.09 $10^{-10}$ | 1.67 $10^{-06}$ | 7.03 $10^{-05}$ |
| LU+3 | 1.19 $10^{-11}$ | -1.19 $10^{-11}$ | 3.87 $10^{-08}$ | 1.63 $10^{-06}$ |
| 264 | 0.0 | 0* | 0* | 0* |

from 4 MOs: HO-1, HO, LU and LU+1.

Yet, as expected the sum over all MOs of the $n_i$ coefficients is not zero, but here amounts to 1.636 $10^{-6}$ electron. From Equation 17, we can then expect $\gamma_i$ to converge to approximately $-3.272\ 10^{-6}$ a.u. for the low-lying MOs (second right-hand term in equation). It may be observed that this is indeed the case, as illustrated for the very first MO. Nevertheless, as in the case of the non-normalised response, frontier MOs bear much larger contributions than any other MO. As such, even though the magnitude of response differs between the normalised and non-normalised schemes, at a qualitative level one may expect them to offer comparable descriptions. This is indeed observed, as shown on Figure 1.

The same analysis holds for the case of the HCN molecule. We give in Table 2 the values for the normalised and non-normalised responses for this molecule at 0.1 Tp (3830 K), for all occupied MOs (HO-6 to HO) and near-frontier vacant MOs (LU to LU+3).

Here also the deviations from the Fermi-Dirac scheme are low (the difference between N and $\langle N \rangle$ is $7.10^{-8}$ electrons only), suggesting the temperature can be considered "low". Conversely the first order response shows larger values, indicating that the effect of temperature is more pronounced at first order. The largest contributions here also arise as expected

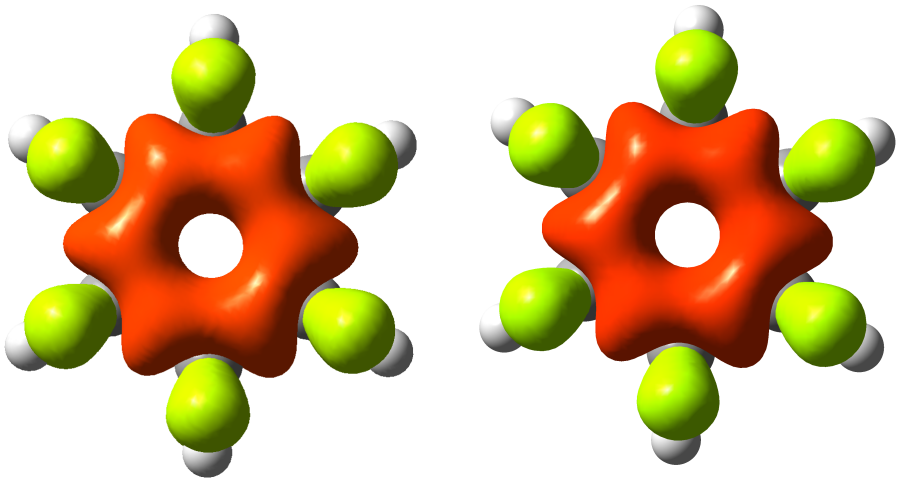

Figure 1: $f_T(\mathbf{r})$ isosurfaces for the benzene molecule at 0.1 $T_p$. Left: non-normalised framework; right, normalised framework. Isovalues: $1.10^{-6}$ a.u. Colour scheme: lime, positive; orange, negative.

from the frontier MOs ($\pi$ HO and HO-1, $\pi^\star$ LU and LU+1). Here too the non-normalised response principally stems from 4 MOs: HO-1, HO, LU and LU+1.

In this case, it may be noted that the sum over all MOs of the $n_i$ coefficients is not zero, but amounts to -9.09 $10^{-5}$ e. The sign of the $\gamma_i$ coefficient for the low-lying MOs will thus be positive and not negative, amounting to 1.82 $10^{-4}$ e. Yet as for benzene the frontier MOs contributions are significantly larger (2 orders of magnitude higher), and thus the normalised and non-normalised density responses are expected to display comparable descriptions at a qualitative level. This is indeed observed, as shown on Figure 2.

## Applications

In the following, we will illustrate on a set of examples how the newly proposed descriptor may help to interpret and rationalise reactivity. All calculations were performed for a temperature $T$ equal to $0.1T_p$. Only the normalised responses will be discussed hereafter.

The examples were chosen in line with those presented by B. Pino-Rios and J. Martinez-Araya,[42] along with additional compounds (*cis* butadiene, $Zn(CH_3)_2$). They comprise compounds exhibiting degenerate frontier levels, as well as systems displaying near-degenerate

Table 2: Results of the temperature-dependent calculation for the HCN molecule à 0.1 $T_p$. FD is the Fermi-Dirac coefficient, $\Delta_{int}$ the difference between the Fermi-Dirac and expected integer MO population, $n_i$ the non-normalised first-order T-derivative of the Fermi-Dirac coefficients, and $\gamma_i$ the normalised response.

| MO | FD | $\Delta_{int}$ | $n_i$ | $\gamma_i$ |
|---|---|---|---|---|
| HO-6 | 2.00 $10^{+00}$ | 0.00 $10^{+00}$ | 0.00 $10^{+00}$ | 1.82 $10^{-04}$ |
| HO-5 | 2.00 $10^{+00}$ | 0.00 $10^{+00}$ | 0.00 $10^{+00}$ | 1.82 $10^{-04}$ |
| HO-4 | 2.00 $10^{+00}$ | 0.00 $10^{+00}$ | -2.20 $10^{-23}$ | 1.82 $10^{-04}$ |
| HO-3 | 2.00 $10^{+00}$ | 0.00 $10^{+00}$ | -2.53 $10^{-12}$ | 1.82 $10^{-04}$ |
| HO-2 | 2.00 $10^{+00}$ | 8.69 $10^{-08}$ | -1.21 $10^{-04}$ | -1.51 $10^{-03}$ |
| HO-1 | 2.00 $10^{+00}$ | 3.96 $10^{-07}$ | -5.03 $10^{-04}$ | -6.86 $10^{-03}$ |
| HO | 2.00 $10^{+00}$ | 3.96 $10^{-07}$ | -5.03 $10^{-04}$ | -6.86 $10^{-03}$ |
| LU | 3.96 $10^{-07}$ | -3.96 $10^{-07}$ | 5.03 $10^{-04}$ | 7.04 $10^{-03}$ |
| LU+1 | 3.96 $10^{-07}$ | -3.96 $10^{-07}$ | 5.03 $10^{-04}$ | 7.04 $10^{-03}$ |
| LU+2 | 1.99 $10^{-08}$ | -1.99 $10^{-08}$ | 3.01 $10^{-05}$ | 4.22 $10^{-04}$ |
| LU+3 | 3.04 $10^{-11}$ | -3.04 $10^{-11}$ | 6.22 $10^{-08}$ | 8.71 $10^{-07}$ |

MOs.

### (Quasi)-Linear molecules

Let us first consider linear or quasi-linear molecules. In Figure 3, we represent isosurfaces of normalised $f_T(\mathbf{r})$ at 0.1 $T_p$, for CO, HCN, $CO_2$, $C_2H_2$, $C_2F_2$ and $Zn(CH_3)_2$.

First, it may be noted that symmetries are correctly taken into account: the response of density is indeed showing a perfect cylindrical symmetry for all linear molecules. In the case of $Zn(CH_3)_2$, a quasi-cylindrical is observed, also in agreement with the molecular geometry. Additionally, for $CO_2$, $C_2H_2$, $C_2F_2$ and $Zn(CH_3)_2$, the molecule should present an inversion center, and satisfactorily, the density response is invariant by inversion in these cases.

But beyond symmetries, the obtained descriptors comply nicely with chemical knowledge. Areas associated with a high electron density, such as triple bonds, lone pairs at electronegative elements (oxygen, nitrogen), basic Lewis sites such as methylide ligand in $ZnMe_2$ are indeed associated to a negative value of $f_T$, characterising nucleophilicity. Conversely, electrophilic regions, like for instance the central C atom in carbon dioxide or the zinc atom in dimethylzinc, appear associated to positive values of $f_T$. It is noteworthy that in the case of

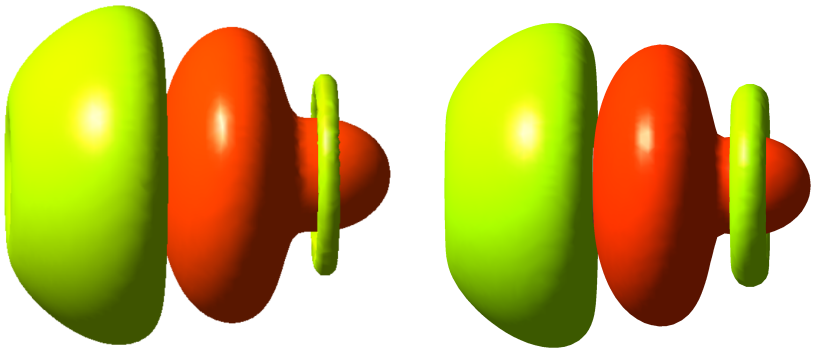

Figure 2: $f_T(\mathbf{r})$ isosurfaces for the HCN molecule at 0.1 $T_p$. Left: non-normalised framework; right, normalised framework. Isovalues: $1.10^{-6}$ a.u. Colour scheme: lime, positive; orange, negative.

CO, we retrieve known coordination features for this species: Lewis basicity on the C atom along the molecular axis, enabling $\sigma$-donation to metal cations, and electrophilicity on the sides of the C-O bond, distorted towards the C atom, enabling $\pi$ retrodonation to CO from metal cations orbitals.[43]

### High symmetry molecules

Similarly, octahedral ($SF_6$, $Cr(CO)_6$), tetrahedral ($P_4O_{10}$) and bipyramid-trigonal ($PCl_5$) symmetries are also respected, as shown in Figure 4.

Here also, chemical properties are retrieved from $f_T$. For instance, the propensity of $PCl_5$ or $P_4O_{10}$ to undergo nucleophilic attack at the P atom can be seen from the electrophilic basins on this atom.[44,45] Similarly, the fact that carbonyl ligands in $Cr(CO)_6$ can be attacked by strong nucleophiles (Grignard reagents, organolithium compounds) can be explained by the large electrophilic domains surrounding these ligands.[46] Activation of $SF_6$ by Lewis base coordination on fluorine atoms is also accounted for by electrophilic basins on these atoms, pointing outside of the molecule.[47]

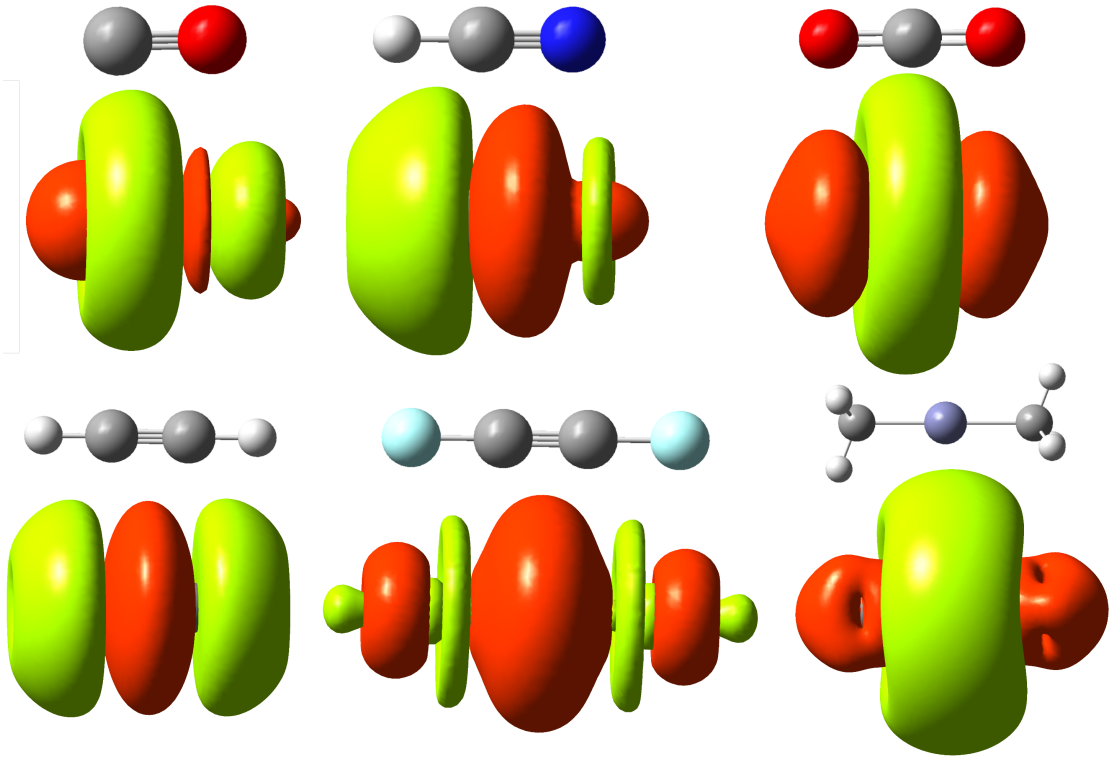

Figure 3: Isosurfaces of the normalised first-order derivative of electron density with respect to temperature for, from top left to bottom right, CO, HCN, $CO_2$, $C_2H_2$, $C_2F_2$, $Zn(CH_3)_2$. Calculation at 0.1 $T_p$. Isovalue: $10^{-6}$ a.u. Colour scheme: lime, positive; orange, negative. Molecular structures are displayed on top of each isosurface to highlight orientation. Atom colour code: gray, C; white, H; red, O; blue, N; cyan, F; lavender, Zn.

### Aromatic molecules

We provide in Figure 5 the normalised $f_T$ isosurfaces for benzene, hexafluorobenzene and $C_{60}$ fullerene, computed at 0.1 $T_p$. Again, symmetry is correctly taken into account. But more interestingly, chemical properties are once again nicely retrieved. For instance, it is textbook knowledge that benzene takes part in aromatic electrophilic substitutions, and accordingly nucleophilic developments are observed on the C atoms along the ring. Conversely, $C_6F_6$ is known to take part in nucleophilic aromatic substitutions, and indeeed electrophilicity is observed on the aromatic ring.[48]

In the case of fullerene, regioselectivity in Diels-Alder reaction can also be rationalised. The addition of a diene is indeed expected to result to the so-called [6,6] addition (reaction with the C-C bond bridging two 6-member rings) rather than [6,5].[49] In Figure 6 we recall

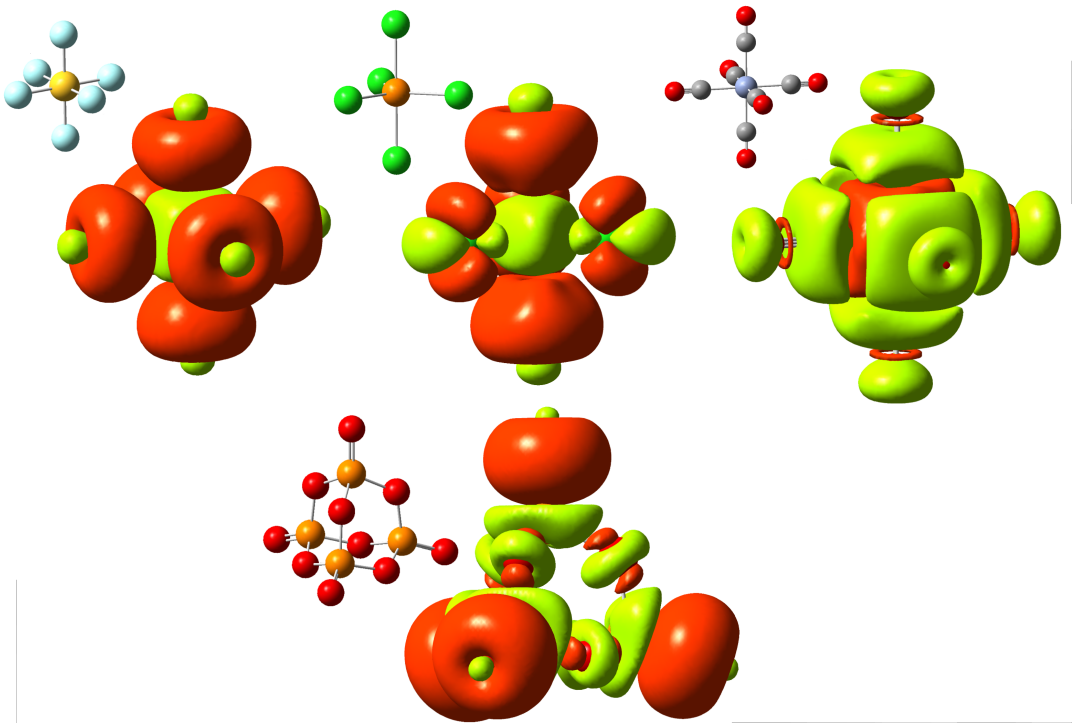

Figure 4: Isosurfaces of the normalised first-order derivative of electron density with respect to temperature for, from top left to bottom right, $SF_6$, $PCl_5$, $Cr(CO)_6$, $P_4O_{10}$. Same isovalue and colour scheme as Figure 3. Atom colour scheme: yellow, S; cyan, F; lavender, Cr; gray, C; red, O; orange, P; green, Cl.

the $f_T$ isosurface for fullerene and compare it with the $10^{-6}$ isosurface of $f_T$ for cis-butadiene. If one only focuses on the interaction of the central electrophilic development of butadiene with nucleophilic regions of fullerene, addition on any C-C bond would appear possible. However, only addition on the [6,6] bonds allows additional stabilising interactions between the nucleophilic basins of butadiene and electrophilic domains on fullerene (within the 5-membered ring). Hence a significant selectivity for this addition is expected, in line with experimental data.

## Conclusion

In this publication, we derived a simple yet efficient reactivity descriptor, stemming from the Fermi-Dirac population scheme applied to SCF MO diagrams. Under the approximation that

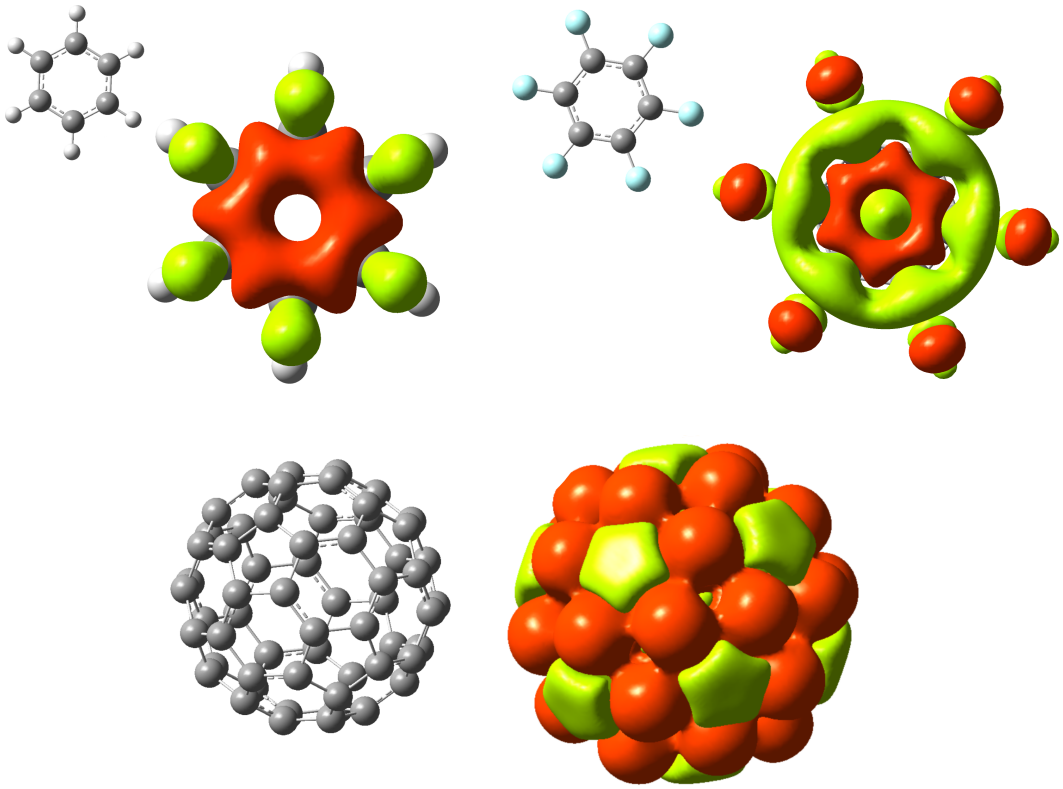

Figure 5: Isosurfaces of the normalised first-order derivative of electron density with respect to temperature for, from top left to bottom right, $C_6H_6$, $C_6F_6$ and $C_{60}$ fullerene. Same colour scheme as Figure 3. Isovalue: $1.10^{-6}$ a.u. for $C_6H_6$ and $C_6F_6$, $1.10^{-7}$ a.u. for $C_{60}$. Atom colour scheme: gray, C; white, H; cyan, F.

MO diagrams only marginally change when temperature is slightly increased from 0 K, we developed the electron density response to changes in temperature, starting from "standard" 0 K DFT calculations. This electron density response develops over the whole set of MOs, but it can be shown that, at low temperatures (which are required for our approximations to hold), the principal contributions stem from frontier levels, in line with Fukui's FMO theory. From there a connection with the Dual Descriptor can be rather directly proposed, supporting the use of this new quantity to probe reactivity and selectivity. Its additional advantages are the natural inclusion of orbital degeneracies, as well as incorporation of non-frontier MOs contributions. We thus implemented the target descriptor, along with a canonical (normalised) counterpart, using a python-based library (Orbkit, cross- quantum chemistry software). We then showed on a set of representative examples the efficiency of

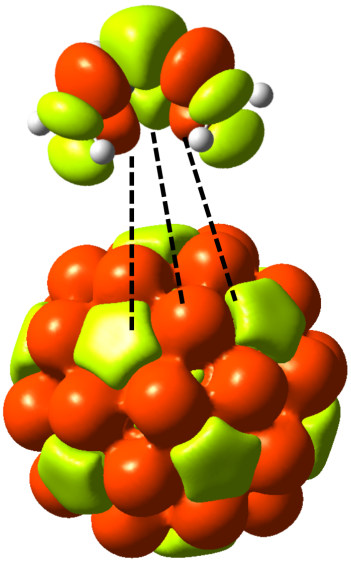

Figure 6: Explanation of the regioselectivity of the butadiene addition on fullerene. Black dashed lines are serve a guide for the eye.

this quantity to indeed retrieve chemical selectivity and reactivity, noticeably on systems for which the FMO approximation is known to misbehave.

On an ending note, during the course of this manuscript redaction a publication was released, dealing with application of C-DFT descriptors in the solid state, noticeably Fukui functions and local softness.[50] These descriptors were evaluated through different formulations, noticeably relying on the Fermi-Dirac population scheme. Difficulties were met in the computation and interpretation of the electrophilic response, related to the large difference in levels density between the conduction and valence bands. Could our proposition offer a solution?

## Supplementary material

Python3/orbkit script, optimised geometries in cartesian coordinate format, post-treatment outputs (text files, detailing MO contributions to the overall response).

## Acknowledgments

The authors wish to thank the referees for their constructive comments and suggestions. They helped enhancing the quality of this publication and opened interesting perspectives on the future of this work.

## References

(1) Ayers, P. W.; Anderson, J. S. M.; Bartolotti, L. J. Perturbative perspectives on the chemical reaction prediction problem. *Int. J. Quantum Chem.* **2005**, *101*, 520–534.

(2) Hammond, G. S. A Correlation of Reaction Rates. *J. Am. Chem. Soc.* **1955**, *77*, 334–338.

(3) Geerlings, P.; De Proft, F.; Langenaeker, W. Conceptual Density Functional Theory. *Chem. Rev.* **2003**, *103*, 1793–1874.

(4) Chermette, H. Chemical reactivity indexes in density functional theory. *J. Comput. Chem.* **1999**, *20*, 129–154.

(5) Geerlings, P.; Chamorro, E.; Chattaraj, P. K.; Proft, F. D.; Gázquez, J. L.; Liu, S.; Morell, C.; Toro-Labbé, A.; Vela, A.; Ayers, P. Conceptual density functional theory: status, prospects, issues. *Theor. Chem. Acc.* **2020**, *139*, 2.

(6) Clarys, T.; Stuyver, T.; De Proft, F.; Geerlings, P. Extending conceptual DFT to include additional variables: oriented external electric field. *Phys. Chem. Chem. Phys.* **2021**, *23*, 990–1005.

(7) Bettens, T.; Alonso, M.; Geerlings, P.; De Proft, F. Implementing the mechanical force into the conceptual DFT framework: understanding and predicting molecular mechanochemical properties. *Phys. Chem. Chem. Phys.* **2019**, *21*, 7378–7388.

(8) Nalewajski, R. F. Internal density functional theory of molecular systems. *J. Chem. Phys.* **1984**, *81*, 2088–2102.

(9) Ghosh, S. K.; Berkowitz, M.; Parr, R. G. Transcription of ground-state density-functional theory into a local thermodynamics. *Proc. Natl. Acad. Sci. U. S. A.* **1984**, *81*, 8028–8031.

(10) Nagy, A.; Parr, R. G. Information entropy as a measure of the quality of an approximate electronic wave function. *Int. J. Quantum Chem.* **1996**, *58*, 323–327.

(11) Chattaraj, P. K.; Cedillo, A.; Parr, R. G. Chemical softness in model electronic systems: dependence on temperature and chemical potential. *Chem. Phys.* **1996**, *204*, 429–437.

(12) Perdew, J. P.; Parr, R. G.; Levy, M.; Balduz, J. L. Density-Functional Theory for Fractional Particle Number: Derivative Discontinuities of the Energy. *Phys. Rev. Lett.* **1982**, *49*, 1691–1694.

(13) Cárdenas, C.; Ayers, P. W.; Cedillo, A. Reactivity indicators for degenerate states in the density-functional theoretic chemical reactivity theory. *J. Chem. Phys.* **2011**, *134*, 174103.

(14) Franco-Pérez, M.; Ayers, P. W.; Gázquez, J. L. Average electronic energy is the central quantity in conceptual chemical reactivity theory. *Theor. Chem. Acc.* **2016**, *135*, 8.

(15) Miranda-Quintana, R. A.; Ayers, P. W. Fractional electron number, temperature, and perturbations in chemical reactions. *Phys. Chem. Chem. Phys.* **2016**, *18*, 15070–15080.

(16) Franco-Pérez, M.; Heidar-Zadeh, F.; Ayers, P. W.; Gázquez, J. L.; Vela, A. Going beyond the three-state ensemble model: the electronic chemical potential and Fukui function for the general case. *Phys. Chem. Chem. Phys.* **2017**, *19*, 11588–11602.

(17) Franco-Pérez, M. An electronic temperature definition for the reactive electronic

species: Conciliating practical approaches in conceptual chemical reactivity theory with a rigorous ensemble formulation. *J. Chem. Phys.* **2019**, *151*, 074105.

(18) Gazquez, J. L.; Franco-Pérez, M.; Ayers, P. W.; Vela, A. Temperature-dependent approach to chemical reactivity concepts in density functional theory. *Int. J. Quantum Chem.* **2019**, *119*, e25797.

(19) Miranda-Quintana, R. A.; Franco-Perez, M.; Gazquez, J. L.; Ayers, P. W.; Vela, A. Chemical hardness: Temperature dependent definitions and reactivity principles. *J. Chem. Phys.* **2018**, *149*, 124110.

(20) Franco-Pérez, M.; Gázquez, J. L.; Ayers, P. W.; Vela, A. Temperature-Dependent Approach to Electronic Charge Transfer. *J. Phys. Chem. A* **2020**, *124*, 5465–5473.

(21) Franco-Pérez, M.; Polanco-Ramirez, C. A.; Gazquez, J. L.; Ayers, P. W.; Vela, A. Study of organic reactions using chemical reactivity descriptors derived through a temperature-dependent approach. *Theor. Chem. Acc.* **2020**, *139*, 44.

(22) Landau, L.; Lifshiftz, E. *Statistical Physics*; Elsevier, 1980; pp 158–190.

(23) Guégan, F.; Tognetti, V.; Martínez-Araya, J. I.; Chermette, H.; Merzoud, L.; Toro-Labbé, A.; Morell, C. A statistical thermodynamics view of electron density polarisation: application to chemical selectivity. *Phys. Chem. Chem. Phys.* **2020**, *22*, 23553–23562.

(24) Parr, R. G.; Yang, W. *Density-Functional Theory of Atoms and Molecules*; International Series of Monographs on Chemistry; Oxford University Press, 1994.

(25) Parr, R. G.; Donnelly, R. A.; Levy, M.; Palke, W. E. Electronegativity: The density functional viewpoint. *J. Chem. Phys.* **1978**, *68*, 3801–3807.

(26) Mermin, N. D. Thermal Properties of the Inhomogeneous Electron Gas. *Phys. Rev.* **1965**, *137*, A1441–A1443.

(27) Bultinck, P.; Cardenas, C.; Fuentealba, P.; Johnson, P. A.; Ayers, P. W. How to Compute the Fukui Matrix and Function for Systems with (Quasi-)Degenerate States. *J. Chem. Theory Comput.* **2014**, *10*, 202–210.

(28) Fukui, K. The Role of Frontier Orbitals in Chemical Reactions (Nobel Lecture). *Angew. Chem. Int. Ed.* **1982**, *21*, 801–809.

(29) Parr, R. G.; Pearson, R. G. Absolute hardness: companion parameter to absolute electronegativity. *J. Am. Chem. Soc.* **1983**, *105*, 7512–7516.

(30) Parr, R. G.; Yang, W. Density functional approach to the frontier-electron theory of chemical reactivity. *J. Am. Chem. Soc.* **1984**, *106*, 4049–4050.

(31) Morell, C.; Grand, A.; Toro-Labbé, A. *J. Phys. Chem. A* **2005**, *109*, 205–212.

(32) De Proft, F.; Ayers, P. W.; Fias, S.; Geerlings, P. Woodward-Hoffmann rules in density functional theory: Initial hardness response. *J. Chem. Phys.* **2006**, *125*, 214101.

(33) Franco-Pérez, M.; Ayers, P. W.; Gázquez, J. L.; Vela, A. Thermodynamic responses of electronic systems. *J. Chem. Phys.* **2017**, *147*, 094105.

(34) Pearson, R. G. Hard and Soft Acids and Bases. *Journal of the American Chemical Society* **1963**, *85*, 3533.

(35) Pearson, R. G. The principle of maximum hardness. *Accounts of Chemical Research* **1993**, *26*, 250–255.

(36) Pino-Rios, R.; Inostroza, D.; Cárdenas-Jirón, G.; Tiznado, W. Orbital-Weighted Dual Descriptor for the Study of Local Reactivity of Systems with (Quasi-) Degenerate States. *J. Phys. Chem. A* **2019**, *123*, 10556–10562.

(37) Cardenas, C.; Munoz, M.; Contreras, J.; Ayers, P. W.; Gomez, T.; Fuentealba, P. Understanding Chemical Reactivity in Extended Systems: Exploring Models of Chemical Softness in Carbon Nanotubes. *Acta Phys.-Chim. Sin.* **2018**, *34*, 631.

(38) Frisch, M. J.; Trucks, G. W.; Schlegel, H. B.; Scuseria, G. E.; Robb, M. A.; Cheeseman, J. R.; Scalmani, G.; Barone, V.; Petersson, G. A.; Nakatsuji, H. et al. Gaussian˜16 Revision B.01. 2016; Gaussian Inc. Wallingford CT.

(39) Kendall, R. A.; Dunning, T. H.; Harrison, R. J. Electron affinities of the first-row atoms revisited. Systematic basis sets and wave functions. *J. Chem. Phys.* **1992**, *96*, 6796–6806.

(40) Stephens, P. J.; Devlin, F. J.; Chabalowski, C. F.; Frisch, M. J. Ab Initio Calculation of Vibrational Absorption and Circular Dichroism Spectra Using Density Functional Force Fields. *J. Phys. Chem.* **1994**, *98*, 11623–11627.

(41) Hermann, G.; Pohl, V.; Tremblay, J. C.; Paulus, B.; Hege, H.-C.; Schild, A. ORBKIT: A modular python toolbox for cross-platform postprocessing of quantum chemical wavefunction data. *J. Comput. Chem.* **2016**, *37*, 1511–1520.

(42) Martínez-Araya, J. I. A generalized operational formula based on total electronic densities to obtain 3D pictures of the dual descriptor to reveal nucleophilic and electrophilic sites accurately on closed-shell molecules. *J. Comput. Chem.* **2016**, *37*, 2279–2303.

(43) Atkins, P.; Overton, T. *Shriver and Atkins' Inorganic Chemistry*; Oxford University Press, 2010.

(44) Wong, C. Y.; Kennepohl, D. K.; Cavell, R. G. Neutral Six-Coordinate Phosphorus. *Chem. Rev.* **1996**, *96*, 1917–1952.

(45) Johansson, S.; Kuhlmann, C.; Weber, J.; Paululat, T.; Engelhard, C.; Schmedt auf der Günne, J. Decomposition of P4O10 in DMSO. *Chem. Commun.* **2018**, *54*, 7605–7608.

(46) Dodson, G. R.; Paxson, J. R. Octahedral metal carbonyls. XXXII. Kinetics and mechanism of reactions of methyllithium with Group VIb metal carbonyls and derivatives in diethyl ether. *J. Am. Chem. Soc.* **1973**, *95*, 5925–5930.

(47) Buß, F.; Mück-Lichtenfeld, C.; Mehlmann, P.; Dielmann, F. Nucleophilic Activation of Sulfur Hexafluoride: Metal-Free, Selective Degradation by Phosphines. *Angew. Chem. Int. Ed.* **2018**, *57*, 4951–4955.

(48) Robson, P.; Stacey, M.; Stephens, R.; Tatlow, J. C. 925. Aromatic polyfluoro-compounds. Part VI. Penta- and 2,3,5,6-tetra-fluorothiophenol. *J. Chem. Soc.* **1960**, 4754–4760.

(49) Fernández, I.; Solà, M.; Bickelhaupt, F. M. Why Do Cycloaddition Reactions Involving C60 Prefer [6,6] over [5,6] Bonds? *Chem. - Eur. J.* **2013**, *19*, 7416–7422.

(50) Deraet, X.; Turek, J.; Alonso, M.; Tielens, F.; Cottenier, S.; Ayers, P. W.; Weckhuysen, B. M.; De Proft, F. Reactivity of Single Transition Metal Atoms on a Hydroxylated Amorphous Silica Surface: A Periodic Conceptual DFT Investigation. *Chem. – Eur. J.* **2021**, *27*, 6050–6063.

Figure 7: TOC graphic.